Elastic Buckling of Moderately Thick Homogeneous Circular Plates of Variable Thickness

S.K. Jalali[*], M.H. Naei

Faculty of Mechanical Engineering, College of Engineering, University of Tehran, Tehran, Iran

ABSTRACT

In this study, the buckling response of homogeneous circular plates with variable thickness subjected to radial compression based on the first-order shear deformation plate theory in conjunction with von-Karman nonlinear strain-displacement relations is investigated. Furthermore, optimal thickness distribution over the plate with respect to buckling is presented. In order to determine the distribution of the prebuckling load along the radius, the membrane equation is solved using the shooting method. Subsequently, employing the pseudospectral method that makes use of Chebyshev polynomials, the stability equations are solved. The influence of the boundary conditions, the thickness variation profile and aspect ratio on the buckling behavior is examined. The comparison shows that the results derived, using the current method, compare very well with those available in the literature.

Keywords: Buckling analysis; Variable thickness circular plates; First-order shear deformation plate theory; Shooting method; Pseudospectral method

1 INTRODUCTION

STABILITY analysis and studies on the buckling behavior of plates have been always considered as one of the important subjects in structural analysis (Timoshenko and Gere [1], Almroth and Brush [2], and Turvey and Marshall [3]). On the other hand, variable thickness plates have always been attractive for designers, and a lot of researches have been done on this subject [4-6]. The most conspicuous usage of variable thickness plates is to lighten structures, especially when used in high-speed aircrafts. With an accurate design of the thickness distribution, one can make an increase in buckling capacity of the plate compared to its uniform thickness counterpart. Wang et al. [7] investigated the elastic buckling of tapered circular plates using the shooting method and the Rayleigh-Ritz approach. Asymmetric vibration and elastic stability of polar orthotropic circular plates of linearly varying thickness subjected to hydrostatic in-plane force are discussed on the basis of classical plate theory using Ritz method by Gupta and Ansari [8]. Dumir and Khatri [9] studied axisymmetric postbuckling of fiber-reinforced cylindrically orthotropic thin tapered circular plates subjected to an in-plane radial compressive and investigated the effect of orthotropic parameter and taper ratio for clamped and simply-supported plates. Özakça et al. [10] carried out the buckling analysis of tapered circular and annular plates using the finite element method. A family of variable thickness, Mindlin-Reissner axisymmetric finite elements has developed which include shear deformation and rotary inertia effects. Shufrin and Eisenberger [11] studied the buckling behavior of thick elastic rectangular plates with variable thickness, applying both the first-order and high-order shear deformation plate theories, using the extended Kantorovich method.

Circular plates are one of the most important elements in structural design. On the other hand, optimum design is a big concern especially in applications such as aerospace, where reducing the structural members' weight is

---

[*] Corresponding author. Tel.: +98 21 6111 4021.
  E-mail address: skjalali@ut.ac.ir (S.K. Jalali).

JOURNAL OF SOLID MECHANICS JSM

essential. Therefore, in this study, the buckling analysis of moderately thick circular plates with variable thickness under radial compression is investigated for clamped and simply supported boundary conditions. The equilibrium and associated stability equations are derived based on the first-order shear deformation plate theory in the von-Karman sense.

2   PROBLEM FORMULATIONS

2.1 Geometry

Consider a circular plate of radius b which is mid-plane symmetric, as shown in Fig. 1. The plate is under radial compression P. The origin of the cylindrical coordinates system lies on the center of the mid-plane where r and z define the radial and thickness directions, φ defines the rotation about the circumferential axis, and u and w are the displacements in r and z directions, respectively. The plate thickness is a function of r as follows

$$h(r) = h_1 + \left(h_2 - h_1 \right) \left(\frac{r}{b} \right)^p \tag{1}$$

where h_1 and h_2 are the thicknesses of the plate at the center and the edge, respectively, and p defines the profile of the thickness. Although the formulation and the method are general for circular plates with any kind of profile through the thickness, the analysis is performed only on plates with linear and parabolic profiles. Considering a plate of constant volume, V, the relationship between the geometrical parameters is given by

$$h_0 = \frac{V}{\pi b^2} = h_1 + \frac{2(h_2 - h_1)}{p+2} \tag{2}$$

$$\Omega = \frac{h_2}{h_1 + h_2} \tag{3}$$

where h_0 is the thickness of its uniform thickness counterpart, and Ω is the taper parameter ranging from 0 to 1, defining the volume distribution of the plate in the radial direction. $\Omega=0$, and 1 correspond to maximum thickness at the center and the edge of the plate, respectively, while $\Omega=0.5$ corresponds to a plate of constant thickness. Some plate sections with various taper parameter and their corresponding h_1 and h_2 values for equal plate volume is presented in Fig. 2.
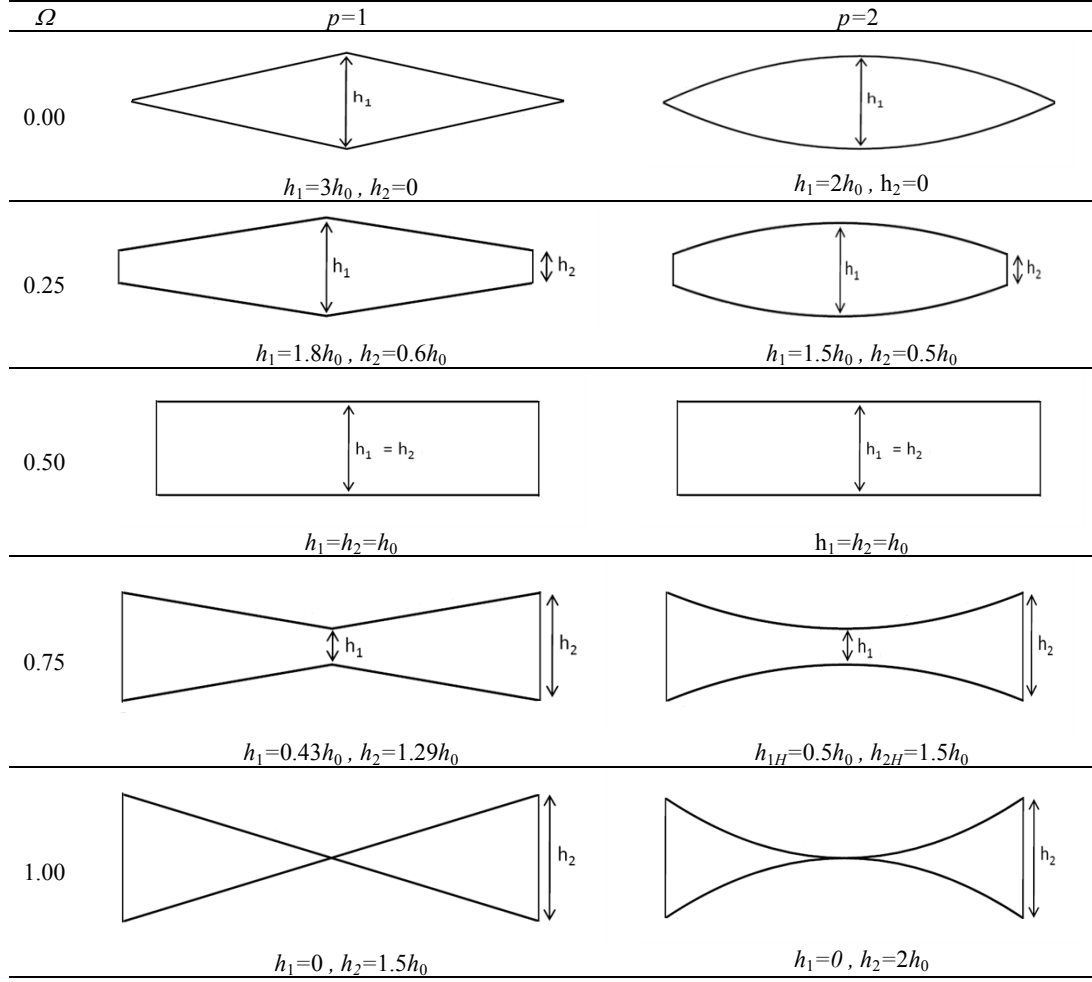
2.2 Equilibrium and stability equations

In order to consider the nonlinear effects of the buckling problem, the axisymmetric strain-displacement relations are written based on von-Karman plate theory

$$\varepsilon_r = \varepsilon_{r0} + k_r z, \qquad \varepsilon_\theta = \varepsilon_{\theta0} + k_\theta z, \qquad \gamma_{rz} = \phi + w_{,r} \tag{4}$$

in which the mid plane strains, ε_{r0} and $\varepsilon_{\theta0}$ are given by
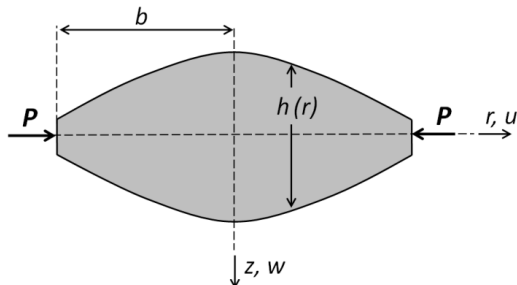
Fig. 1
Geometrical definition of a circular plate with variable thickness.

Ω	$p=1$	$p=2$
0.00		
	$h_1=3h_0$, $h_2=0$	$h_1=2h_0$, $h_2=0$
0.25		
	$h_1=1.8h_0$, $h_2=0.6h_0$	$h_1=1.5h_0$, $h_2=0.5h_0$
0.50		
	$h_1=h_2=h_0$	$h_1=h_2=h_0$
0.75		
	$h_1=0.43h_0$, $h_2=1.29h_0$	$h_{1H}=0.5h_0$, $h_{2H}=1.5h_0$
1.00		
	$h_1=0$, $h_2=1.5h_0$	$h_1=0$, $h_2=2h_0$

Fig. 2
Plate sections for various values of taper parameter Ω and corresponding values of h_1 and h_2.

$$\varepsilon_{r0}=u_{,r}+\frac{1}{2}(w_{,r})^2, \qquad \varepsilon_{\theta0}=\frac{u}{r} \tag{5}$$

and the curvatures, k_r and k_θ are defined as

$$k_r=\phi_{,r}, \qquad k_\theta=\frac{\phi}{r} \tag{6}$$

where $(\ )_{,r}$ indicate the differentiation with respect to r. The relations between stress and strain are based on Hook's law.

$$\sigma_r=\frac{E}{1-v^2}(\varepsilon_r+v\varepsilon_\theta), \qquad \sigma_\theta=\frac{E}{1-v^2}(\varepsilon_\theta+v\varepsilon_r), \qquad \tau_{rz}=\frac{E}{2(1+v)}\gamma_{rz} \tag{7}$$

where σ_r and σ_θ are normal stresses in r- and θ- directions, respectively; and τ_{rz} is the shear stress acting on r=Constant plane and in z-direction. The resultant forces and moments of the stresses are given by

$$(N_r, N_\theta) = \int_{-h(r)/2}^{h(r)/2} (\sigma_r, \sigma_\theta)\, dz \tag{8a}$$

$$(M_r, M_\theta) = \int_{-h(r)/2}^{h(r)/2} (\sigma_r, \sigma_\theta) z\, dz \tag{8b}$$

$$Q_r = K \int_{-h(r)/2}^{h(r)/2} \tau_{rz}\, dz \tag{8c}$$

where K is the shear correction coefficient in the first-order shear deformation plate theory, which is set to 5/6. Substituting Eq. (7) into Eq. (8) results in the following relations between resultant forces and moments and the strains

$$\begin{pmatrix} N_r \\ N_\theta \end{pmatrix} = A_{11} \begin{bmatrix} 1 & v \\ v & 1 \end{bmatrix} \begin{pmatrix} \varepsilon_{r0} \\ \varepsilon_{\theta 0} \end{pmatrix} \tag{9a}$$

$$\begin{pmatrix} M_r \\ M_\theta \end{pmatrix} = D_{11} \begin{bmatrix} 1 & v \\ v & 1 \end{bmatrix} \begin{pmatrix} k_r \\ k_\theta \end{pmatrix} \tag{9b}$$

$$Q_r = A_{55}\, \gamma_{rz} \tag{9c}$$

$$(A_{11}, D_{11}) = \int_{-h(r)/2}^{h(r)/2} (1, z^2) \frac{E}{1-v^2}\, dz, \qquad A_{55} = \frac{K A_{11}(1-v)}{2} \tag{10}$$

Equilibrium equations of the circular plate with axisymmetric deformations can be obtained using stationary potential energy method as follows [2]

$$N_{r,r} + \frac{N_r - N_\theta}{r} = 0 \tag{11a}$$

$$Q_r + rQ_{r,r} + (rN_r w_{,r})_{,r} = 0 \tag{11b}$$

$$M_{r,r} + \frac{M_r - M_\theta}{r} - Q_r = 0 \tag{11c}$$

Substituting Eqs. (4)-(6) and (9) into Eq. (11) gives the equilibrium equations in terms of the displacement components

$$A_{11} w_{,r} w_{,rr} + \frac{1}{2r}(A_{11}(1-v) + r A_{11,r}) w_{,r}^2 + A_{11} u_{,rr} + \frac{1}{r}\, A_{11} + r A_{11,r}\; u_{,r}$$
$$+ \frac{1}{r}\left(v A_{11,r} - \frac{A_{11}}{r} \right) u = 0 \tag{12a}$$

$$w_{,rr}\left(A_{55} + A_{11}\left(u_{,r} + \frac{3}{2}(w_{,r})^2 + v\frac{u}{r} \right) \right) + w_{,r}\left(A_{55,r} + \frac{A_{55}}{r} + \left(\frac{A_{11}}{r}(1+v) + A_{11,r} \right) u_{,r} \right)$$
$$+ \frac{1}{2}(A_{11} + r A_{11,r})(w_{,r})^2 + v A_{11,r}\frac{u}{r} + A_{11} u_{,rr} + A_{55}\phi_{,r} + \left(A_{55,r} + \frac{A_{55}}{r} \right)\phi = 0 \tag{12b}$$

$$D_{11}\varphi_{,rr} + \frac{1}{r}(D_{11} + r D_{11,r})\varphi_{,r} - \frac{1}{r}\left(\frac{D_{11}}{r} - v D_{11,r} + r A_{55} \right)\varphi - A_{55} w_{,r} = 0 \tag{12c}$$

One can obtain all the configurations of the plate from the above equation. There are two types of equilibrium configurations possible for a plate under in-plane loading, which are undeflected and buckled configurations. When buckling happens, the plate configuration will turn from the undeflected configuration into the buckled one. The intersection of these two equilibrium configurations is called the bifurcation point. This point can be obtained by solution of linear differential equations of stability. The linear equations of stability necessary for this process may be derived from the nonlinear equilibrium equations, Eq. (12), by use of a perturbation technique in which the displacement field, (u, w, φ), is replaced by $(u_0+u_1, w_0+w_1, \varphi_0+\varphi_1)$, where (u_0, w_0, φ_0) represents an equilibrium configuration in the undeflected state, and (u_1, w_1, φ_1) is a small increment. This method is called adjacent equilibrium criterion (from Almroth and Brush [2]). Therefore, the stability equations can be expressed as

$$A_{11} u_{1,rr} + \frac{1}{r}(A_{11} + r A_{11,r}) u_{1,r} - \frac{1}{r^2}(A_{11} - \nu r A_{11,r}) u_1 = 0 \tag{13a}$$

$$(A_{55} + N_{r0}) w_{1,rr} + \frac{1}{r}(A_{55} + N_{r0} + r(A_{55,r} + N_{r0,r})) w_{1,r} + A_{55} \phi_{1,r} + \frac{1}{r}(A_{55} + r A_{55,r}) \phi_1 = 0 \tag{13b}$$

$$D_{11} \phi_{1,rr} + \frac{1}{r}(D_{11} + r D_{11,r}) \phi_{1,r} - \frac{1}{r^2}(D_{11} - \nu r D_{11,r} + r^2 A_{55}) \phi_1 - A_{55} w_{1,r} = 0 \tag{13c}$$

The stability equations are homogenous and linear and have solutions only for discrete values of the applied load, which refers to an eigenvalue problem. The smallest eigenvalue is termed the critical buckling load P_{cr}. It should be noticed that Eq. (13a) is decoupled from the Eqs. (13b) and (13c). The boundary conditions for the stability equations are

$$\phi_1 = 0, \qquad w_{1,r} = 0 \qquad \text{Center} \tag{14a}$$

$$w_1 = 0, \qquad \phi_1 = 0 \qquad \text{Clamped} \tag{14b}$$

$$w_1 = 0, \qquad M_r = D_{11}\left(\phi_{1,r} + \frac{\nu}{b}\phi_1\right) = 0 \qquad \text{Simply Supported} \tag{14c}$$

In Eq. (13) N_{r0} is the prebuckling load, which must be obtained from the equilibrium equations of the plate. But since the plate is in its undeflected configuration, w_0 and φ_0 are equal to zero, and the equilibrium Eq. (12) can be revised into the following equation called the membrane equation

$$A_{11} u_{0,rr} + \frac{1}{r}(A_{11} + r A_{11,r}) u_{0,r} - \frac{1}{r^2}(A_{11} - \nu r A_{11,r}) u_0 = 0 \tag{15}$$

Solving the above equation, u_0 may be obtained and therefore, N_{r0} can be calculated from Eq. (9a). The boundary conditions for membrane equation can be expressed as

$$u_0 = 0 \qquad \text{Center} \tag{16a}$$

$$N_{r0} = A_{11}\left(u_{0,r} + \frac{\nu}{r}u_0\right) = -P \qquad \text{Edge} \tag{16b}$$

3   NUMERICAL SOLUTION METHODS
3.1 Shooting method

The shooting method, consisting of the well known Runge-Kutta method in conjunction with a Newton-Raphson iterative formulation, is employed to numerically solve the membrane equation, Eq. (15). Taking Eq. (16a) and assuming an initial value for $u_{0,r}$, the membrane equation is solved using Runge-Kutta method. The Newton-Raphson formulation is then applied to iterate the initial value of $u_{0,r}$ in a way that the answers satisfy the boundary condition, Eq. (16b), at the edge of the plate.

3.2 Pseudospectral method

The pseudospectral method is employed to numerically solve the eigenvalue problem, Eqs. (13) and (14). The basic idea in this method is to assume that the answer of the differential equations can be approximated by a sum of finite number of basic functions with unknown coefficients. The pseudospectral method demands that the differential equation be exactly satisfied at a set of points known as the collocation points. Usually when the solution is not especially periodic, Chebyshev polynomials are the best choices as basic functions (from Boyd [12]). Chebyshev polynomials are of great use for eigenvalue problems of plates e.g. [13]. These polynomials can be expressed by the following recursive equation

$$T_1 = 1 \tag{17a}$$

$$T_2 = x \tag{17b}$$

$$T_{n+1} = 2xT_n - T_{n-1} \tag{17c}$$

To approximate the answers with Chebyshev polynomials, the solution range should be changed from $r \in [0,b]$ to $x \in [-1,1]$. For this purpose, r is substituted with x based on the following equations

$$x = \frac{2r}{b} - 1, \qquad \mathrm{d}x = \frac{2}{b}\mathrm{d}r \tag{18}$$

The following dimensionless parameters are introduced to make the stability equations dimensionless

$$x_1 = \frac{w_1}{b}, \quad x_2 = \varphi_1, \quad \overline{N}_{r0} = \frac{N_{r0}}{A_{55}}, \quad \overline{N}'_{r0} = \frac{b\,N_{r0,r}}{2\,A_{55}}, \quad \overline{A}'_{55} = \frac{b\,A_{55,r}}{2A_{55}}, \quad \overline{D}'_{11} = \frac{b\,D_{11,r}}{2D_{11}}, \quad \overline{F} = \frac{b^2 A_{55}}{D_{11}} \tag{19}$$

where x_1 and x_2 are dimensionless transverse displacement and rotation about the radial axis, respectively. Therefore, the stability equations, Eq. (13), and the boundary conditions, Eq. (14), can be rewritten in the following form, where ( ) shows the derivative with respect to x

$$2(\overline{N}_{r0}+1)x_1'' + 2\left[\frac{(\overline{N}_{r0}+1)}{(x+1)} + (\overline{A}'_{55}+\overline{N}_{r0})\right]x_1' + x_2' + \left[\frac{1}{(x+1)} + \overline{A}'_{55}\right]x_2 = 0 \tag{20a}$$

$$2x_2'' + 2\left[\frac{1}{(x+1)} + \overline{D}'_{11}\right]x_2' - 2\left[\frac{1}{(x+1)^2} - \frac{v\,\overline{D}'_{11}}{(x+1)} + \frac{\overline{F}}{4}\right]x_2 - \overline{F}x_1' = 0 \tag{20b}$$

$$x_1'(-1) = 0, \qquad x_2(-1) = 0 \qquad\qquad \text{Center} \tag{21a}$$

$$x_1(1) = 0, \qquad x_2(1) = 0 \qquad\qquad \text{Clamped} \tag{21b}$$

$$x_1(1) = 0, \qquad \left(x_2'(1) + \frac{v}{2}x_2(1)\right) = 0 \qquad \text{Simply Supported} \tag{21c}$$

where x_1 and x_2 are approximated by a sum of $n+1$ Chebyshev polynomials as follows

$$x_{1i} = \sum_{j=1}^{n+1} a_j T_{i,j} \tag{22a}$$

$$x_{2i} = \sum_{j=1}^{n+1} b_j T_{i,j} \tag{22b}$$

where indexes i and j refer to the ith collocation point and the jth Chebyshev polynomial, respectively, and a_j and b_j are unknown coefficients. In order to solve the equations, $2n+2$ algebraic equations are needed. The boundary conditions, Eq. (21), provide four of the required equations. Besides, satisfying Eqs. (20a) and (20b) in $n-1$ collocation points supplies $2n-2$ remained algebraic equations. To minimize the error, based on the Gauss-Lobatto interpolation points, the optimal collocation points can be selected as follows

$$x_i = \cos\left(\frac{\pi i}{N-2}\right), \qquad i = 0,1,2,\cdots, N-2 \tag{23}$$

The results are represented in dimensionless form using the buckling load factor λ defined by

$$\lambda = \frac{P_{cr}b^2}{D_0}, \qquad D_0 = \frac{E_m h_0^3}{12(1-v^2)} \tag{24}$$

4   NUMERICAL RESULTS AND DISCUSSIONS

In the following, numerical results of the buckling behavior of clamped (C) and simply supported (SS) circular plates with variable thickness under radial compression are presented. Thickness variation is considered to be either linear or parabolic taper. As the determination of prebuckling load distribution along the plate radius is a prerequisite for solving the stability equations, the derived results from the membrane equation should be verified at first. The results are compared with those presented by Wang et al. [7] in terms of stress function f. The comparison would be possible using the relationship between the prebuckling load and the stress function as follows

$$f = r N_{r0} \tag{25a}$$

$$\bar{f} = \frac{f}{bP} \tag{25b}$$

in which $\bar{f}$ is the dimensionless parameter of the stress function. Variations of $\bar{f}$ with respect to the dimensionless parameter of radial coordinate r/b for various taper parameters are shown in Fig. 3. It shows that the results are of a good accuracy. For the purpose of verifying the buckling behavior, at first a comparison study for thick circular plates with constant thickness is made with those obtained by Wang et al. [14] using Rayleigh-Ritz energy approach, Raju and Rao [15] using Galerkin's method, and Özakça [10] applying FEM in Table 1. Then verification is carried out for the buckling behavior of circular plates with variable thickness.
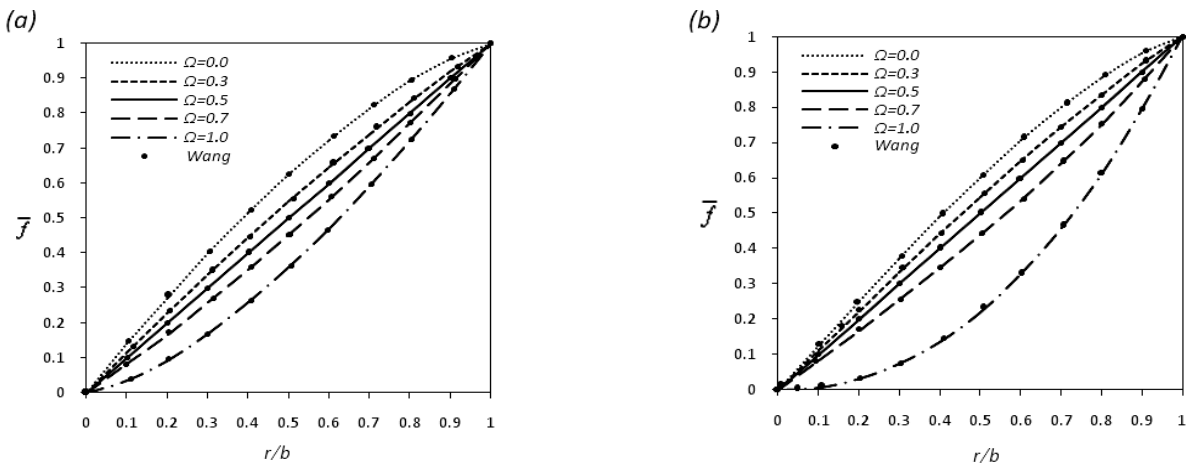

Fig. 3
Variations of dimensionless parameter of the stress function $\bar{f}$ with respect to dimensionless parameter of radial coordinate r/b,
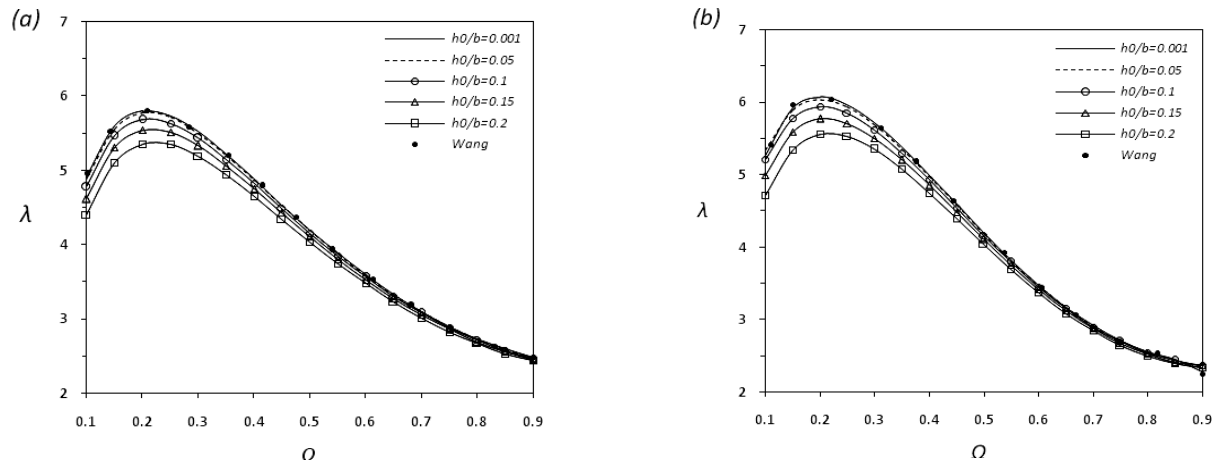(a): Linear taper; (b): Parabolic taper.

Table 1
Comparisons of the present buckling load factors λ with previous results available in the literature

	Source	h_0/b			
		0.001	0.05	0.1	0.2
C	Present	14.6819	14.5296	14.0909	12.5724
	Ref. [14]	14.6819	14.5296	14.0909	12.5725
	Ref. [15]	14.6825	14.5299	14.0910	12.5725
	Ref. [10]	14.6819	14.5014	13.9885	12.2843
	Ref. [1]	14.6842	14.6842	14.6842	14.6842
SS	Present	4.1978	4.1852	4.1480	4.0056
	Ref. [14]	4.1978	4.1853	4.1480	4.0056
	Ref. [15]	4.1978	4.1852	4.1481	4.0056
	Ref. [10]	4.1978	4.1844	4.1448	3.9938
	Ref. [1]	4.2025	4.2025	4.2025	4.2025

Figs. 4 and 5 show the variations of the buckling factor λ with respect to taper parameter Ω. The results are presented for various values of aspect ratio h_0/b and are compared with the results obtained by Wang et al. [7] using Rayleigh-Ritz method based on classic plate theory. It is seen that the buckling factor λ decreases with increasing the aspect ratio h_0/b due to the increasing transverse shear deformation. This phenomenon is not supported by classic plate theory.
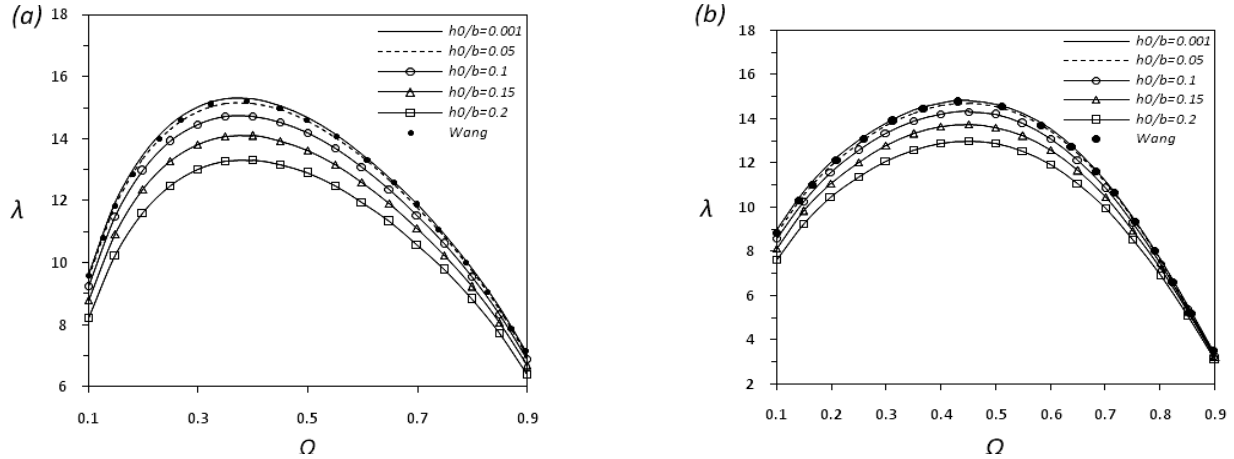
Fig. 4
Buckling load factor λ with respect to taper parameter Ω for clamped edge, (a): Linear taper; (b): Parabolic taper.

Fig. 5
Buckling load factor λ with respect to taper parameter Ω for simply supported edge, (a): Linear taper; (b): Parabolic taper.

Table 2
Optimal values of taper parameter Ω and the buckling load factor λ of homogenous circular plates with variable thickness for specified values of aspect ratio h_0/b

			Wang et al. [7]	h_0/b			
				0.001	0.1	0.15	0.2
C	Linear	Ω_{opt}	0.374	0.374	0.377	0.382	0.387
		λ_{opt}	15.2973	15.2978	14.6417	13.8975	12.9755
	Parabolic	Ω_{opt}	0.446	0.447	0.447	0.447	0.448
		λ_{opt}	14.8335	14.8337	14.2325	13.5462	12.6893
SS	Linear	Ω_{opt}	0.210	0.210	0.214	0.218	0.225
		λ_{opt}	5.8082	5.8062	5.6694	5.5080	5.2994
	Parabolic	Ω_{opt}	0.197	0.198	0.204	0.211	0.220
		λ_{opt}	6.0807	6.0894	5.9090	5.7187	5.4766

Furthermore, it is found that there exists an optimal value for taper parameter Ω, for which the buckling factor λ is maximum. Optimal values of taper parameter Ω and corresponding buckling factor λ for clamped and simply supported boundary conditions are presented in Table 2.

5   CONCLUSION

The buckling behavior of moderately thick circular plates with variable thickness under radial compression based on the first-order shear deformation plate theory and nonlinear von-Karman displacement field is studied. Numerical solution for both clamped and simply supported boundary conditions and for either linear or parabolic taper is presented. For the purpose of verifying the accuracy of the results, the critical buckling load is compared with the previous researches for both constant and variable thickness plates. The comparison shows that the results derived using the current method compare very well with them. Analyzing the effect of the taper parameter Ω on the buckling load factor λ shows that there exists an optimal value for taper parameter Ω, for which the buckling factor λ is maximum. Optimal values of taper parameter Ω for clamped and simply supported boundary conditions and for either linear or parabolic taper are presented.

REFERENCES

[1]   Timoshenko S.P., Gere J.M., 1961, *Theory of Elastic Stability*, McGraw-Hill, New York, Second Edition.
[2]   Brush D.O., Almroth B.O., 1975, *Buckling of Bars, Plates and Shells*, McGraw-Hill, New York.
[3]   Turvey G.J., Marshall I.H., 1995, *Buckling and Postbuckling of Composite Plates*, Chapman & Hall, London, First Edition.
[4]   Turvey G.J., 1987, Axisymmetric snap buckling of imperfect, tapered circular plates, *Computers & Structures* **9**: 551-558.
[5]   Raju K.K., Rao G.V., 1985, Post-buckling of cylindrically orthotropic linearly tapered circular plates by finite element method, *Computers & Structures* **21**(5): 969-972.
[6]   Mizusawa T., 1993, Buckling of rectangular Mindlin plates with tapered thickness by the Spline Strip method, *International Journal of Solids and Structures* **30**(12): 1663-1677.
[7]   Wang C.M., Hong G.M., Tan T.J., 1995, Elastic buckling of tapered circular plates, *Computers & Structures* **55**(6): 1055-1061.
[8]   Gupta U.S., Ansari A.H., 1998, Asymmetric vibrations and elastic stability of polar orthotropic circular plates of linearly varying profile, *Journal of Sound and Vibration* **215**(2): 231-250.
[9]   Dumir P.C., Khatri K.N., 1984, Axisymmetric postbuckling of orthotropic thin tapered circular plates, *Fibre Science and Technology* **21**: 233-245.
[10]   Özakça M., Taysi N., Kolcu F., 2003, Buckling analysis and shape optimization of elastic variable thickness circular and annular plates-I. Finite element formulation, *Engineering Structures* **25**: 181-192.
[11]   Shufrin I., Eisenberger M., 2005, Stability of variable thickness shear deformable plates-First order and high order analyses, *Thin-Walled Structures* **43**: 189-207.
[12]   Boyd J.P., 2000, *Chebyshev and Fourier Spectral Methods*, Dover, New York.
[13]   Lee J., Schultz W.W., 2004, Eigenvalue analysis of Timoshenko beams and axisymmetric Mindlin plates by the pseudospectral method, *Journal of Sound and Vibration* **269**: 609-621.
[14]   Wang C.M., Xiang Y., Kitipornchai S., Liew K.M., 1993, Axisymmetric buckling of circular Mindlin plates with ring supports, *Journal of Structural Engineering* **119**: 782-793.
[15]   Raju K.K., Rao G.V., 1983, Finite element analysis of post-buckling behavior of cylindrical orthotropic circular plates, *Fibre Technology* **19:** 145–154.